Bistatic Dual-Polarization Scattering from Rain and Hail at S- and C-Band Frequencies

K. AYDIN, S. H. PARK, AND T. M. WALSH

Department of Electrical Engineering, The Pennsylvania State University, University Park, Pennsylvania

(Manuscript received 7 August 1997, in final form 7 November 1997)

ABSTRACT

Bistatic dual-polarization radar parameters at S- and C-band frequencies are simulated for rain and hail. The goal is to determine their potential for discriminating the two precipitation types and for estimating the parameters of an exponential size distribution for hail. Raindrops and hailstones are modeled as oblate spheroids with canting distributions representing their fall behavior. Three hailstone composition models are used to illustrate the effects of melting. Most of the bistatic radar parameters are significantly affected by the amount of liquid water in the hailstones, which may prove useful in determining the melting level from the vertical profiles of these parameters. For single-polarized transmission, such as vertical (v) or horizontal (h) polarization, the four bistatic radar parameters of interest are effective reflectivity factor (Z_v or Z_h), bistatic-to-backscattering reflectivity ratio (BBR_v or BBR_h), linear depolarization ratio (LDR_v or LDR_h), and magnitude of the correlation coefficient between the co- and cross-polarized signals (ρ_v or ρ_h). If the transmission is dual polarized, then in addition to these two sets of parameters, the bistatic differential reflectivity (Z_{DR}) and the magnitude of the copolarized correlation coefficient (ρ_{hv}) will be available. For low elevation angles of the transmitter and receiver the parameters resulting from h-polarized transmission may be difficult to measure near the bistatic azimuth angle of 90° due to very low signal levels. This may not be an issue for precipitation involving large hailstones.

When parameter pairs such as (LDR_v, ρ_v) and (BBR_v, Z_v) are plotted, it is observed that rain and hail tend to cluster in different regions on these planes. This indicates a potential for using bistatic radar parameters for differentiating rain from hail. Similar pairs are possible for h-polarization. Various other combinations of these parameters lead to similar results. The use of more than one pair of parameters and/or several bistatic receiver locations should enhance the level of confidence in the discrimination process. It should also be noted that in some cases there are regions on these planes where rain and hail overlap and discrimination may not always be possible.

Other than Z_v and Z_h, all of the bistatic radar parameters mentioned above are in the form of ratios. As a result, given an exponential size distribution, $N_0 \exp(-3.67D/D_0)$, they depend only on the median volume diameter D_0 and not on N_0. Assuming that the amount of liquid water and ice in the composition of the hailstones are known, the ratio parameters may be used for estimating D_0. However, among these parameters only BBR_v and BBR_h are negligibly affected by variations in the axial ratio and the mean orientation of hailstones, making them preferable for D_0 estimation. Once D_0 is obtained, N_0 may be estimated using Z_v or Z_h.

1. Introduction

An S-band (10-cm wavelength) bistatic radar system consisting of a monostatic (transmitter and receiver collocated) radar and a remotely located nonscanning bistatic receiver has been successfully demonstrated for measuring dual-Doppler vector wind fields (Wurman et al. 1993; Wurman et al. 1994; Wurman 1994). In this system, the transmitter and both receivers operate at a single polarization. It is of interest to determine the information that may be obtained about the hydrometeors in the scattering volume if the bistatic receiver is dual polarized. Dual-linear-polarization measurements with a monostatic radar have been effective in differentiating liquid and ice phase hydrometeors, detecting hail, and estimating rainfall rate (Seliga and Bringi 1976, 1978; Bringi et al. 1984; Bringi et al. 1986a; Bringi et al. 1986b; Goddard et al. 1982; *Radio Science*, special issue, 1984, Vol. 19, Issue 1; Jameson 1985; Aydin et al. 1986; Aydin et al. 1990; Aydin and Zhao 1990; Illingworth et al. 1986; Vivekanandan et al. 1990; Balakrishnan and Zrnić 1990a,b; Zrnić et al. 1993a; Zrnić et al. 1993b; Doviak and Zrnić 1993).

Bistatic radar systems have previously been investigated for use in observing clouds, precipitation, and clear air echoes (Atlas et al. 1968; Eccles and Rogers 1968; Doviak and Weil 1972; Crane 1974; Shupyatsky 1974; Olsen and Lammers 1978; Awaka and Oguchi 1982a,b; Dibbern 1987). Of particular interest are the work on the use of polarization in bistatic radar systems. Shupyatsky (1974) proposed depolarization measure-

Corresponding author address: Dr. Kultegin Aydin, Department of Electrical Engineering, The Pennsylvania State University, 314 Electrical Engineering East, University Park, PA 16802.
E-mail: k-aydin@psu.edu

TABLE 1. Dielectric constants of raindrops and hailstones at S-band (2.75 GHz) and C-band (5.55 GHz) frequencies.

Particle	ϵ_r (C band)	ϵ_r (S band)
Rain, 5°C	68.38–*j*33.45	80.89–*j*19.92
Dry hail (100% ice), 0°C	3.17–*j*0.002	3.17–*j*0.004
Slightly wet hail (90% ice, 10% water), 0°C	7.52–*j*2.58	8.63–*j*1.63
Wet hail (70% ice, 30% water), 0°C	17.14–*j*8.30	20.71–*j*5.23

ments at various bistatic angles for differentiating large particles from smaller ones (relative to the wavelength). He reported successfully tracing the formation of large particles in cumulonimbus development with such measurements. Awaka and Oguchi (1982a,b) calculated bistatic radar reflectivities of raindrops at 5.33, 14.3, and 34.8 GHz for studying the interference caused by rain between two communication links operating at the same frequency. Based on the work of Shupyatsky (1974), they explored the idea of measuring the drop size distribution aloft using co- and cross-polarized reflectivities. They decided that bistatic azimuth angles near 90° and vertically polarized transmission would provide the best observations for this purpose. Dibbern (1987) also focused on bistatic scattering from rain. He investigated the relationships between median drop diameter and radar parameters such as differential reflectivity, and linear and circular depolarization ratios at various bistatic angles. Based on calculations and measurements at 33 GHz with a continuous wave (CW) bistatic radar, he concluded that scattering angles at 90°–100° were best suited for investigating rainfall, including the estimation of the drop size distribution.

This paper presents results from a computational study of bistatic scattering from rain and hail at 10.9-cm (S-band) and 5.4-cm (C-band) wavelengths. These are the most common frequency bands used around the world for observing weather phenomena. The potential of bistatic polarimetric radar parameters for differentiating rain and hail and estimating hailstone size distribution will be investigated.

2. Rain and hail models

Raindrops and hailstones are both modeled as oblate spheroids. The size-dependent equilibrium axial ratios of raindrops are calculated using Green's formula (Green 1975). Since there is no established relationship for hailstones, their axial ratios are assumed to be independent of size with a value of 0.8 (Knight 1986). The effects of changing the axial ratio to 0.7 and 0.9 are also considered.

The orientation of an oblate spheroid is determined by the polar and azimuthal angles of its symmetry axis, assuming the vertical direction to be the *z* axis and the origin to be at the spheroid's center. For both raindrops and hailstones the azimuthal angle is assumed to be uniformly distributed between 0° and 360°. Their polar angles are assumed to have a Gaussian distribution. For raindrops, which are known to be highly oriented, a mean value of 0° and a standard deviation of 5° is used. For hailstones, which may wobble and gyrate as they fall (Knight and Knight 1970; Roos and Carte 1973; List et al. 1973; Kry and List 1974; Matson and Huggins 1980), a mean value of 0° (90° is considered later in section 5) and a standard deviation of 30° is used. A 45° standard deviation did not lead to any significant changes in the radar parameters compared to 30°.

The raindrop and hailstone temperatures are assumed to be 5° and 0°C, respectively. Both dry (solid ice) and melting (ice–water mixture) hailstones are considered. The melting hailstones are modeled as mixtures of 90% ice–10% water and 70% ice–30% water (percentages based on volume), and for convenience they will be referred to as ''slightly wet'' and ''wet,'' respectively. The dielectric constants for ice and water are determined at 10.9- and 5.4-cm wavelengths (Ray 1972) and the Maxwell–Garnet theory is used to calculate the average dielectric constants for the spongy hailstones (Bohren and Battan 1982). A summary of the dielectric constants is given in Table 1.

The exponential size distribution $N(D) = N_0 \exp(-\Lambda D)$ is used for both rain and hail, where D is the equivolume spherical diameter of a particle. The median volume diameter $D_0 \cong 3.67/\Lambda$. The maximum sizes of raindrops and hailstones are chosen as 8 and 50 mm, respectively. The specific raindrop size distribution model used here is for thunderstorms (Joss et al. 1968) with $N_0 = 1400\ \text{mm}^{-1}\ \text{m}^{-3}$ and $\Lambda = 3R^{-0.21}\ \text{mm}^{-1}$, where R is the rainfall rate in millimeters per hour. Here, Λ is varied from 1.14 to 3 mm^{-1}, which corresponds to R over the range 1–100 mm h^{-1} and D_0 from about 1.2 to 3.2 mm. For hail the model suggested by Cheng and English (1982) is used with $N_0 = 115\Lambda^{3.63}\ \text{mm}^{-1}\ \text{m}^{-3}$. Here, Λ is varied between 0.15 to 0.8 mm^{-1}, which corresponds to D_0 ranging from about 4.5 to 24 mm.

3. Bistatic radar parameters

The bistatic scattering computations for a single particle are performed with the T-matrix method, originally known as the extended boundary condition method (Waterman 1969). Following a notation similar to that of Doviak and Zrnic (1993), the scattering amplitude matrix of a single particle relates the incident (i) field to the scattered (s) field in a given bistatic direction as

$$\begin{bmatrix} E_{\text{v}}^{s} \\ E_{\text{h}}^{s} \end{bmatrix} = \begin{bmatrix} S_{\text{vv}} & S_{\text{vh}} \\ S_{\text{hv}} & S_{\text{hh}} \end{bmatrix} \begin{bmatrix} E_{\text{v}}^{i} \\ E_{\text{h}}^{i} \end{bmatrix} \frac{e^{-jk_o r}}{r}, \tag{1}$$

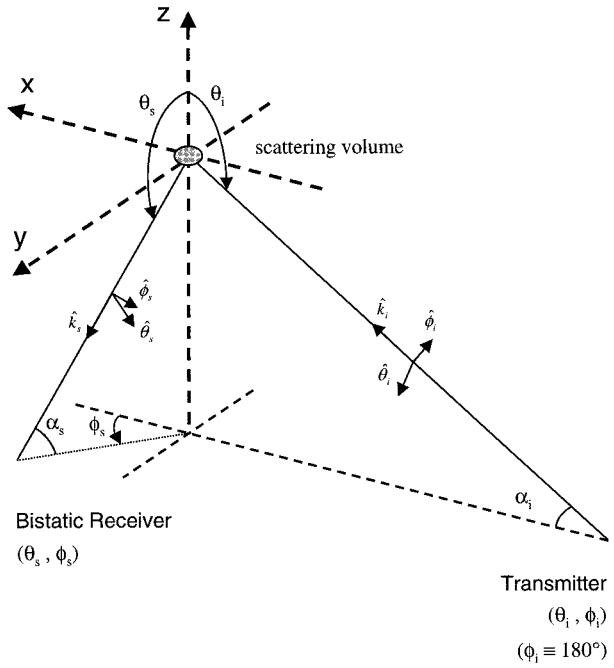

FIG. 1. Bistatic scattering geometry. Here, $\hat{k}_i$ and $\hat{k}_s$ denote the incident and scattering wave directions, respectively. Also, $\alpha_i = \theta_i - 90°$ and $\alpha_s = \theta_s - 90°$ are the transmitter and receiver elevation angles, respectively.

where the harmonic time dependence $\exp(j\omega t)$ is assumed and the first and second subscripts of the matrix elements denote the polarization of the scattered and the incident fields, respectively. Also, $k_0 = 2\pi/\lambda_0$, where λ_0 is the free space wavelength in millimeters. The bistatic radar cross sections of these particles are related to the scattering amplitude matrix elements in (1) as

$$\sigma_{pq} = 4\pi|S_{pq}|^2 \text{ (mm}^2\text{)} \qquad p = \text{v, h and } q = \text{v, h.} \quad (2)$$

The bistatic radar parameters of interest are the effective reflectivity factors at horizontal (h) and vertical (v) polarizations

$$Z_{\text{v}} = C\langle\sigma_{\text{vv}}\rangle \text{ (mm}^6\text{ m}^{-3}\text{)}, \quad (3a)$$

and

$$Z_{\text{h}} = C\langle\sigma_{\text{hh}}\rangle \text{ (mm}^6\text{ m}^{-3}\text{)}; \quad (3b)$$

the bistatic-to-backscattering reflectivity ratios (Aydin and Park 1996; Park 1996)

$$\text{BBR}_{\text{v}} = \frac{\langle\sigma_{\text{vv}}\rangle}{\langle\sigma_{\text{vv}}(180°)\rangle}, \quad (3c)$$

and

$$\text{BBR}_{\text{h}} = \frac{\langle\sigma_{\text{hh}}\rangle}{\langle\sigma_{\text{hh}}(180°)\rangle}; \quad (3d)$$

and linear depolarization ratios

$$\text{LDR}_{\text{v}} = \frac{\langle\sigma_{\text{hv}}\rangle}{\langle\sigma_{\text{vv}}\rangle}, \quad (3e)$$

and

$$\text{LDR}_{\text{h}} = \frac{\langle\sigma_{\text{vh}}\rangle}{\langle\sigma_{\text{hh}}\rangle}; \quad (3f)$$

the cross-polarized correlation coefficients

$$\rho_{\text{v}} = \frac{|\langle S_{\text{hv}}S_{\text{vv}}^*\rangle|}{[\langle|S_{\text{vv}}|^2\rangle\langle|S_{\text{hv}}|^2\rangle]^{1/2}}, \quad (3g)$$

and

$$\rho_{\text{h}} = \frac{|\langle S_{\text{vh}}S_{\text{hh}}^*\rangle|}{[\langle|S_{\text{hh}}|^2\rangle\langle|S_{\text{vh}}|^2\rangle]^{1/2}}; \quad (3h)$$

the differential reflectivity

$$Z_{\text{DR}} = \frac{\langle\sigma_{\text{hh}}\rangle}{\langle\sigma_{\text{vv}}\rangle}; \quad (3i)$$

and the copolarized correlation coefficient

$$\rho_{\text{hv}} = \frac{|\langle S_{\text{vv}}S_{\text{hh}}^*\rangle|}{[\langle|S_{\text{hh}}|^2\rangle\langle|S_{\text{vv}}|^2\rangle]^{1/2}}, \quad (3j)$$

where $C = \lambda_0^4/(\pi^5|K_w|^2)$ and $|K_w|^2 \cong 0.93$ for water at S- and C-band frequencies (Battan 1973). Here $\sigma_{\text{vv}}(180°)$ and $\sigma_{\text{hh}}(180°)$ denote the backscattering cross sections. The brackets $\langle\ \rangle$ denote averaging over the size and orientation distributions, and the symbol * indicates complex conjugation. Hailstones from 1 to 50 mm in 1-mm intervals and raindrops from 0.1 to 8 mm in 0.1-mm intervals were used for integration over the size distribution. Integration over the polar and azimuthal canting angles were performed with 4.5° and 3° step intervals, respectively.

With a bistatic radar system that transmits a single polarization and receives two orthogonal polarizations, only four of the parameters in (3) would potentially be measurable. For v-polarized transmission these are Z_{v}, BBR_{v}, LDR_{v}, and ρ_{v}, and for h-polarized transmission they are Z_{h}, BBR_{h}, LDR_{h}, and ρ_{h}. If the transmission

→

FIG. 2. S-band (10.9-cm wavelength) scattering parameters of a raindrop (solid line) with $D = 4$ mm and axial ratio 0.773, and hailstones with $D = 16$ mm and axial ratio 0.8; dry hailstone (100% ice, dotted line), slightly wet hailstone (10% water–90% ice, dot–dashed line), and wet hailstone (30% water–70% ice, dashed line). The raindrop and the hailstones have their symmetry axes along the vertical direction (z axis).

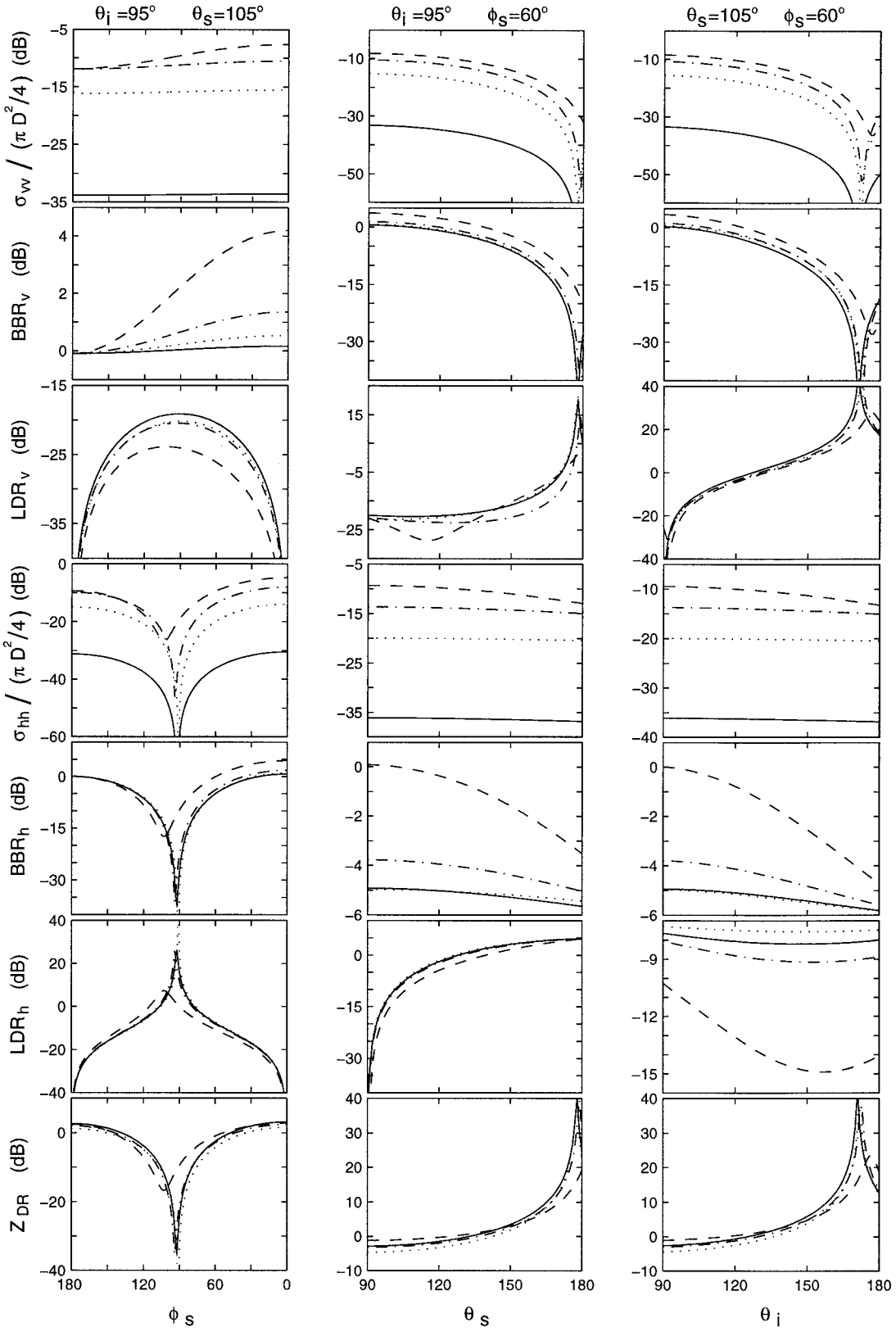

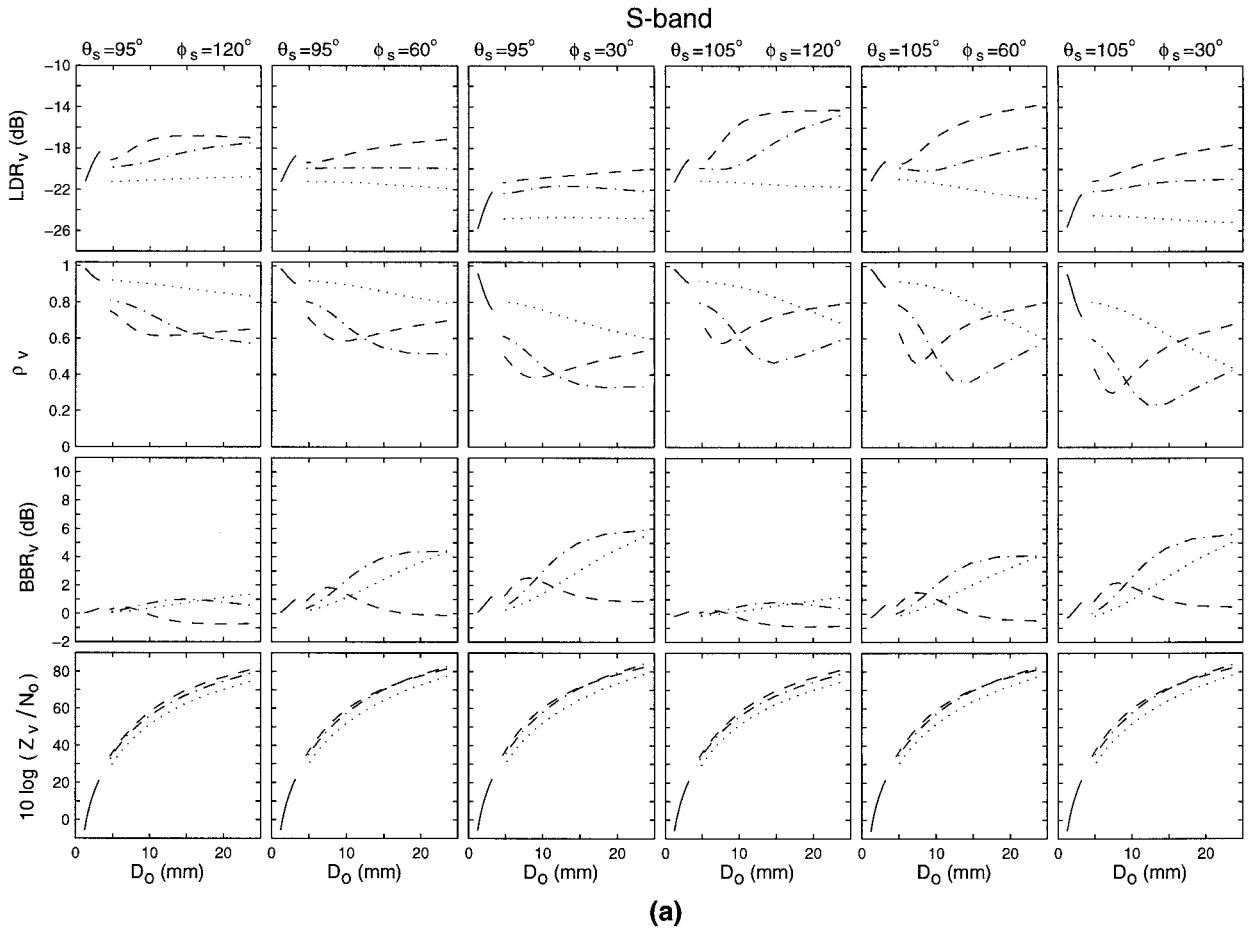

FIG. 3. S-band bistatic radar parameters for (a) v-polarized and (b) h-polarized transmission as a function of the median volume diameter D_0 for an exponential size distribution. The incidence angles are $\theta_i = 95°$ and $\phi_i = 180°$. The curves correspond to rain (solid line), dry hail (dotted line), slightly wet hail (dot–dashed line), and wet hail (dashed line).

is dual polarized, then in addition to these eight parameters, Z_{DR} and ρ_{hv} would also be measurable.

Each radar parameter in (3) depends on the incidence angles (θ_i, ϕ_i) of the transmitted radiation and the bistatic scattering angles (θ_s, ϕ_s). These angles are measured in a coordinate system with the z axis along the vertical direction, the origin centered in the radar resolution volume, and the incidence azimuth angle $\phi_i = 180°$ (Fig. 1). This indicates that the backscattering direction is $\theta_s = \theta_i$, $\phi_s = 180°$. It is clear that there are innumerable possibilities for sets of incidence and scattering angles. Several selected angles will be used to illustrate the characteristics of the radar parameters considered in this study.

4. Scattering from single particles

Before discussing the radar parameters that involve averaging over orientation and size distributions, it is worthwhile to observe some single scattering parameters of the raindrop and hailstone models with their symmetry axes along the vertical direction. These results should be useful in gaining insight into the behavior of radar parameters for various combinations of angles other than those used in the next section. Figure 2 shows S-band ($\lambda_0 = 10.9$ cm) results for a raindrop with equivolume spherical diameter $D = 4$ mm and axial ratio 0.773 and for three hailstone models (dry, slightly wet, and wet) of the same size and shape, with $D = 16$ mm and axial ratio 0.8. Consider the normalized size parameter $X = |m|k_0D/2$, where m is the index of refraction of the homogeneous particle. Here, $X = 0.82$, 1.05, 1.37, and 2.13 for dry hail, raindrop, slightly wet hail, and wet hail, respectively. None of these cases strictly fall into the Rayleigh scattering regime, which requires that $X \ll 1$; however, the raindrop and dry hail models exhibit features resembling Rayleigh scattering.

For the 4-mm raindrop, σ_{vv} and BBR_v change very little as the azimuth angle varies from the backward to the forward direction (first column in Fig. 2), while a large dip in both σ_{hh} and BBR_h occurs at $\phi_s = 90°$, and both are nearly symmetric about this angle. On the other hand, σ_{vv} and BBR_v for the hailstones steadily increase from the backward to the forward direction (Bohren and

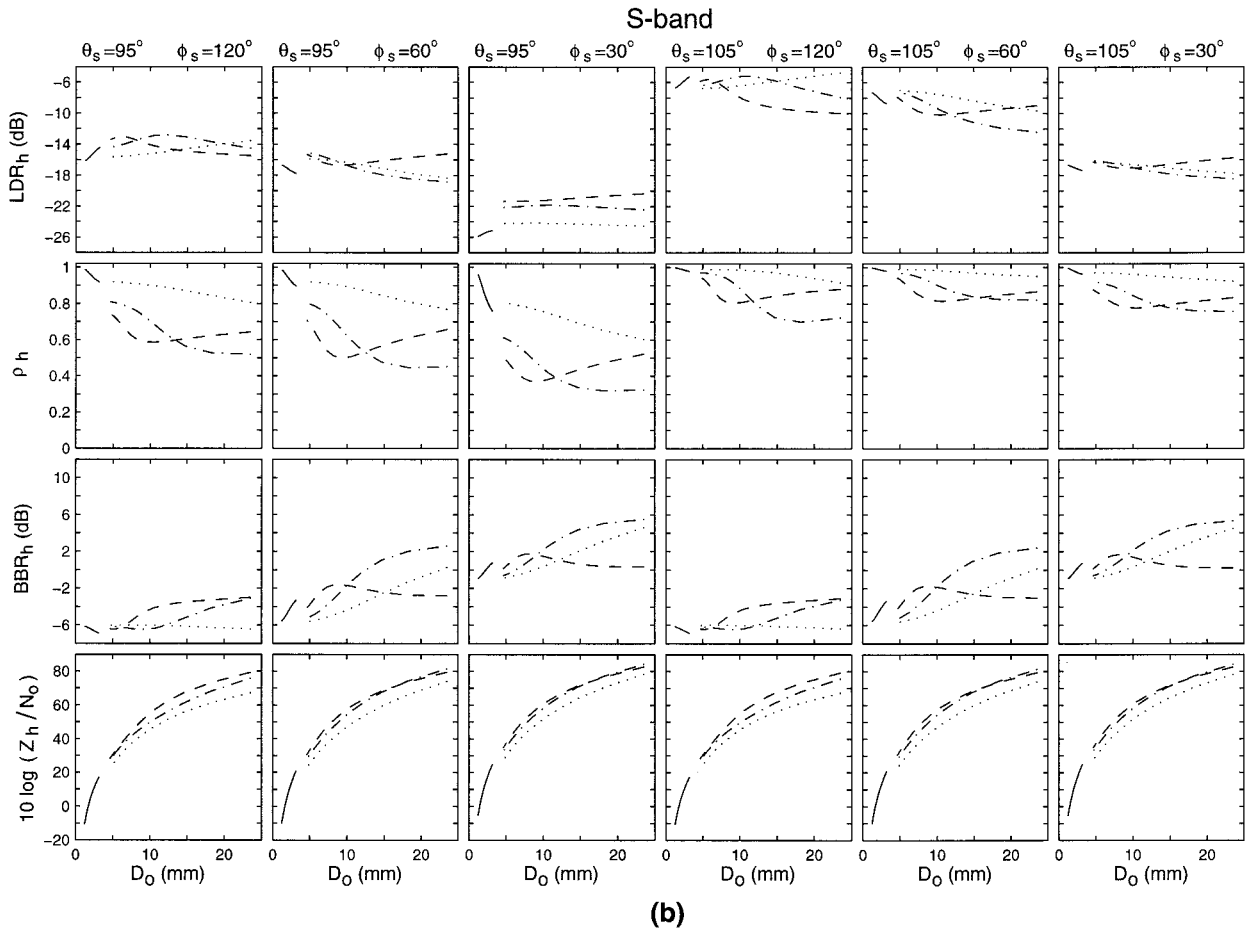

FIG. 3. (*Continued*)

Huffman 1983); this is more pronounced for the wet hailstones, which have larger dielectric constants compared to the dry ones. Also, the dip in both σ_{hh} and BBR_h is not as deep as that of the raindrop (except for the dry hailstone model) and is shifted in the backward direction. Since the oblate spheroidal particles are not canted, LDR_v and LDR_h are equal to 0 ($-\infty$ dB) on the $\phi_s = 0°$ and 180° planes that include the forward and backward scattering directions (Chylek 1977). Both LDRs reach a peak near $\phi_s = 90°$; this peak shifts to the backward direction with increasing size parameter X. The peak in LDR_h is mainly due to the dip in σ_{hh}, which can create difficulty in its measurement at this angle if small particles (including raindrops and dry hail) fill the scattering volume. Here, Z_{DR} follows the combined trends of σ_{hh} and σ_{vv}, with a dip near $\phi_s = 90°$. Also note that all of these parameters are significantly affected by the degree of wetness of the hailstones.

The observed dips in σ_{vv} and BBR_v, and peaks in LDR_v and Z_{DR}, as a function of the scattering polar angle (second column in Fig. 2) and incident polar angle (third column in Fig. 2), are a result of the relative orientation of the incident wave and the observed scattered wave polarizations. For $\theta_s = 105°$ and $\phi_s = 60°$ LDR_v is very sensitive to changes in θ_i when $\theta_i < 120°$ (i.e., $\alpha_i < 30°$), whereas LDR_h is not. On the other hand, for $\theta_i = 95°$ and $\phi_s = 60°$ LDR_h is much more sensitive to θ_s when $\theta_s < 120°$ compared to LDR_v.

Most of the trends observed at S band are also present at C band (not shown here). However, since the model hydrometeors are larger compared to the wavelength at C band, resonance scattering characteristics are dominant. The dips and peaks are smoother and shift to the backward direction with increasing size parameter X, which corresponds to increasing wetness of the hailstone; however, the shift reverses to the forward direction for hail with the largest X. Also, note that at S-band BBR_v and BBR_h increase as the hailstone becomes more wet. However, at C-band BBR_v and BBR_h increase going from dry to slightly wet hailstones and decrease as the hailstone becomes more wet.

5. Scattering from rain and hail

Figures 3–5 show the S- and C-band radar parameters as a function of the median volume diameter D_0 for

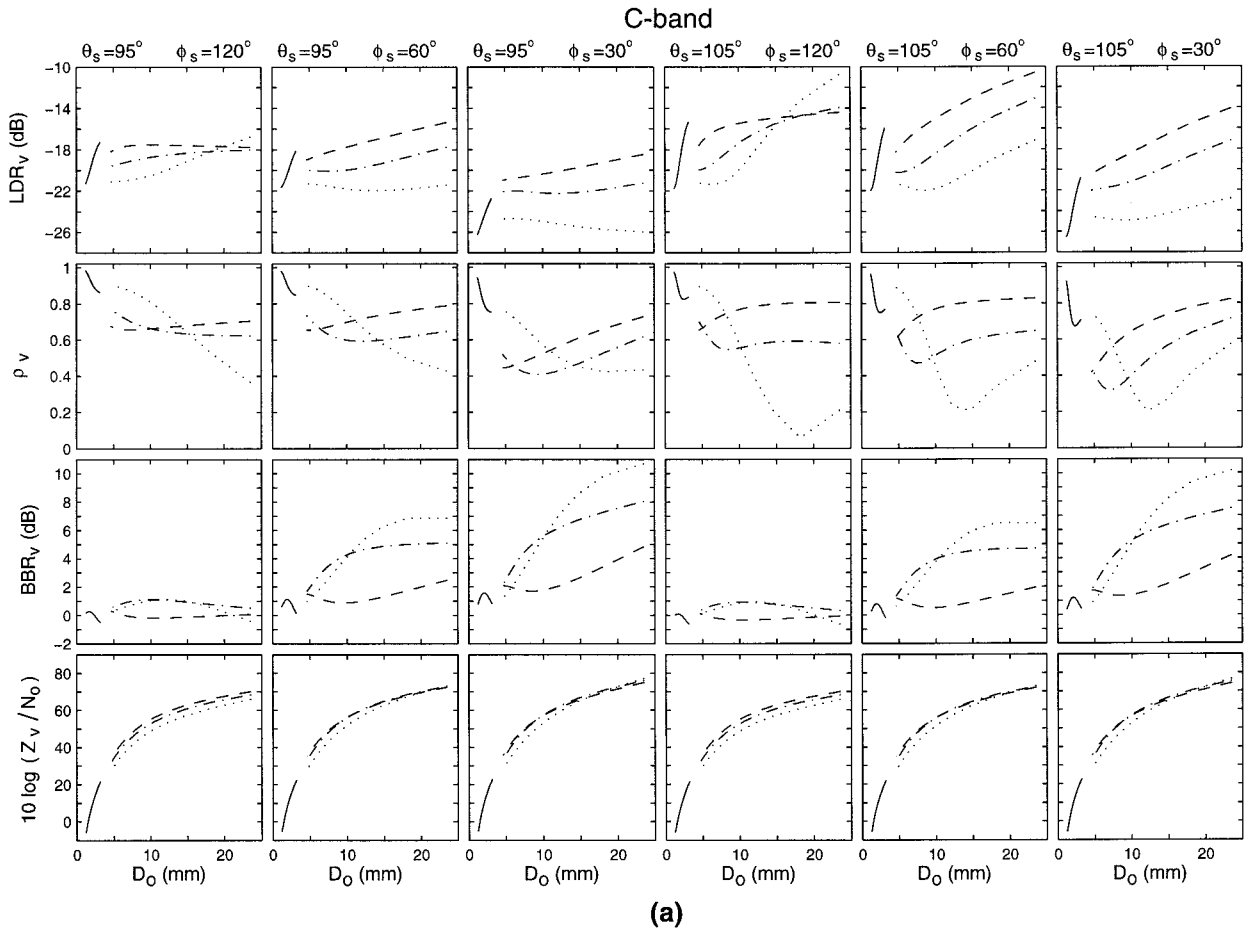

FIG. 4. C-band bistatic radar parameters for (a) v-polarized and (b) h-polarized transmission as a function of the median volume diameter D_0 for an exponential size distribution. The incidence angles are $\theta_i = 95°$ and $\phi_i = 180°$. The curves correspond to rain (solid line), dry hail (dotted line), slightly wet hail (dot–dashed line), and wet hail (dashed line).

several scattering angles with the incidence angles set to $\theta_i = 95°$ and $\phi_i = 180°$. The first three columns in each figure correspond to $\theta_s = 95°$ and three scattering azimuth angles ϕ_s: one in the backward quadrant at 120°, and two in the forward quadrant at 60° and 30°. The last three columns have $\theta_s = 105°$ with the same ϕ_s values. All of these parameters are significantly different in the backward and forward quadrants, especially BBR_v and BBR_h. Note that as D_0 increases, the effects of larger particles in the size distribution become significant. For example, S-band BBR_v and BBR_h increase with D_0 for dry and slightly wet hail, but for wet hail they reach a peak value near $D_0 = 7.5$ mm and decrease afterward; at C band this peak occurs below 5 mm and is not seen in these graphs. The copolarized parameters (BBR_v, BBR_h, Z_v, Z_h, Z_{DR}, and ρ_{hv}) are not affected as much as the cross-polarized parameters (LDR_v, LDR_h, ρ_v, and ρ_h) by the change in θ_s from 95° to 105°, which corresponds to a 10° increase in the bistatic elevation angle α_s (Fig. 1). Most of these parameters are significantly affected by the degree of wetness of the hailstones; as a result, the transition from dry hailstones to wet hailstones may be observable in the vertical profiles of some of these parameters.

Figure 6 shows plots of cross-polarized parameters LDR_v–ρ_v and LDR_h–ρ_h, and copolarized parameters Z_v–BBR_v, Z_h–BBR_h. Note that rain and hail generally lie in different parts of these planes, which may be useful for differentiating them. These clustering regions will be different for each set of incidence and scattering angles. In some cases there are regions where rain and hail are very close or overlapping; as a result, discrimination may not always be possible. Furthermore, Z_{DR} and ρ_{hv} (not shown here) may be useful in differentiating only the largest hail from rain. It should be noted that other combinations of these parameters may also be used for discrimination purposes.

Figure 7 illustrates the effects of hailstone axial ratios on the bistatic radar parameters. Three axial ratios are considered: 0.9, 0.8, and 0.7 (note that the results thus far were for an axial ratio of 0.8). It is clear that BBR_v, BBR_h, Z_v, and Z_h are the least affected compared to the other parameters. Parameters Z_{DR}, LDR_v, and LDR_h increase, while ρ_{hv}, ρ_v, and ρ_h decrease with decreasing

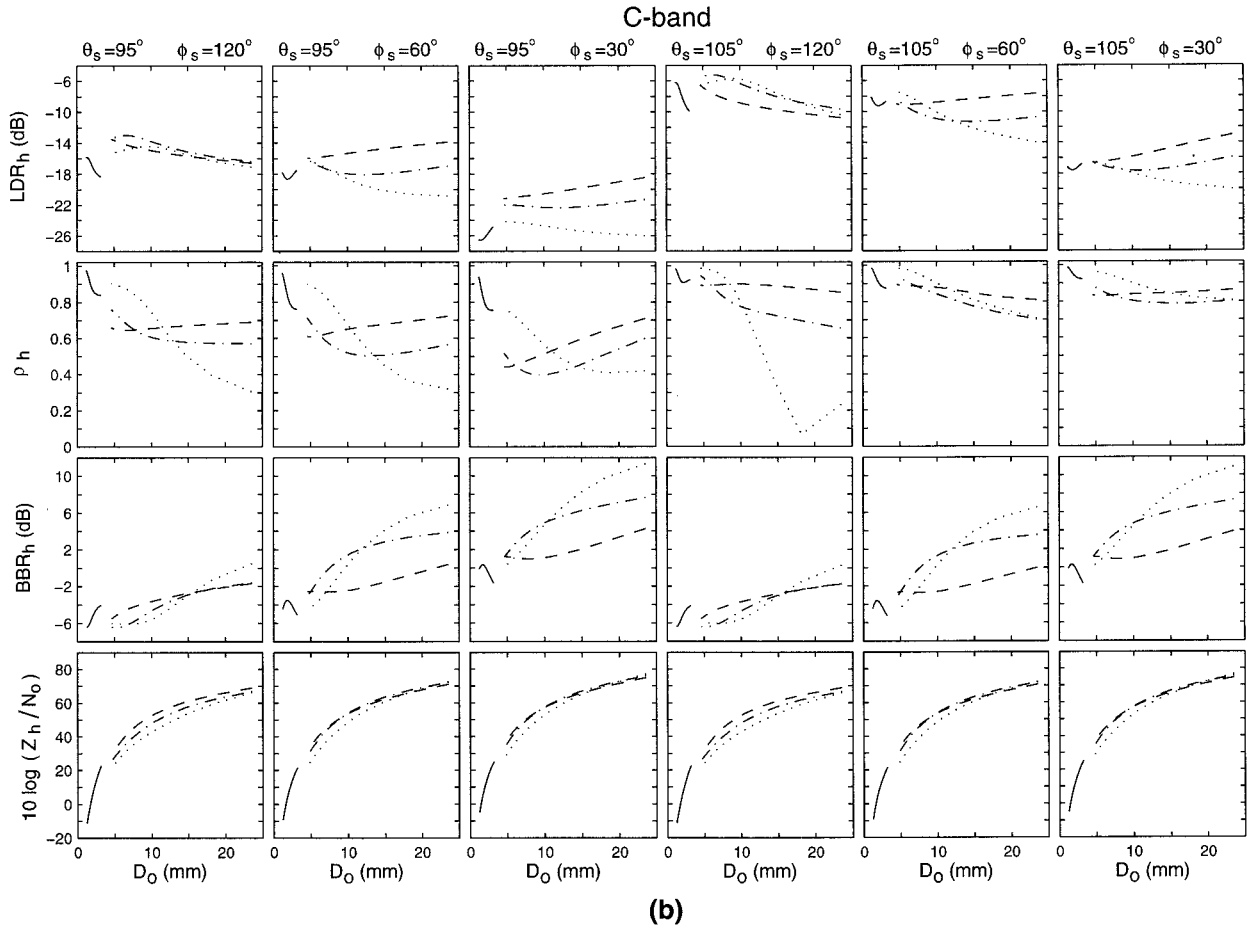

FIG. 4. (*Continued*)

axial ratio. In these plots, as the axial ratio decreases from 0.9 to 0.8, or 0.8 to 0.7, the increases in LDR_v and LDR_h range between 0.5 and 3 dB while the decrease in ρ_v and ρ_h varies between 5% and 30%. The increase in Z_{DR} is about 0.5 dB and changes very little with D_0. Note that BBR_v and BBR_h are not significantly affected (less than 0.5 dB) by changes in the axial ratio.

Figure 8 shows the effects of rotating the mean polar canting angle of the hailstones by 90°; in other words, the symmetry axis, which corresponds to the smaller dimension of an oblate spheroid, becomes parallel to the horizontal plane. In all the previous figures, the symmetry axis was aligned (on average) with the vertical direction. With the symmetry axis rotated 90° the vertical polarization becomes parallel to the larger dimension of the hailstones, whereas the horizontal polarization becomes parallel to both the large and the small dimensions because of the symmetry axis being randomly orientated on the horizontal plane (see section 2). Note that the effect of this orientation change for the hailstones is negligibly small on all the parameters except LDR_v, ρ_v and Z_{DR}. This is mainly due to the larger change in the scattering of the vertically polarized wave compared to the horizontally polarized wave.

The radar parameters in the form of ratios, (3c)–(3j), are functions of D_0 and are independent of N_0, which may make them useful for estimating D_0. For monostatic radars, Seliga and Bringi (1976) used Z_{DR} and its sensitivity to the size-dependent axial ratios of raindrops to estimate D_0, which together with Z_h produced an estimate of N_0. Awaka and Oguchi (1982a) suggested the use of bistatic LDR_v and Z_v measurements in rain for the same purpose. The two parameters (D_0 and N_0) of an exponential size distribution for hail may be estimated if its dielectric constant can be assessed. The location within a storm may provide insight into whether or not the hail is dry or has begun melting. As noted earlier, most of these radar parameters change significantly when hail starts melting and acquires liquid water; this may be observable in their vertical profiles. For a given size distribution, BBR_v and BBR_h are the only parameters that are negligibly affected by both the axial ratio and the orientation of (wet or dry) hailstones and may be preferable for estimating D_0 (see Figs. 4–7). Note that in

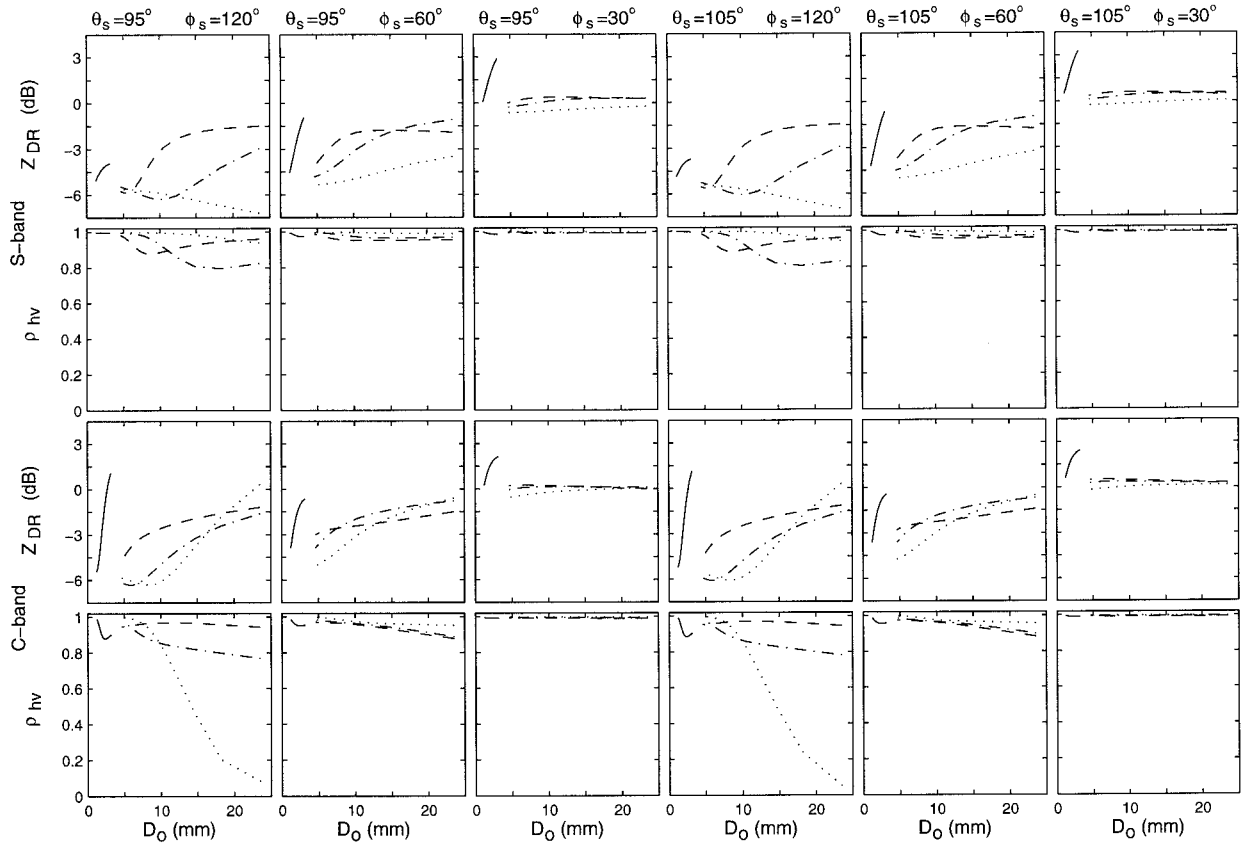

FIG. 5. S- and C-band bistatic radar parameters for dual-polarized transmission as a function of the median volume diameter D_0 for an exponential size distribution. The incidence angles are $\theta_i = 95°$ and $\phi_i = 180°$. The curves correspond to rain (solid line), dry hail (dotted line), slightly wet hail (dot–dashed line), and wet hail (dashed line).

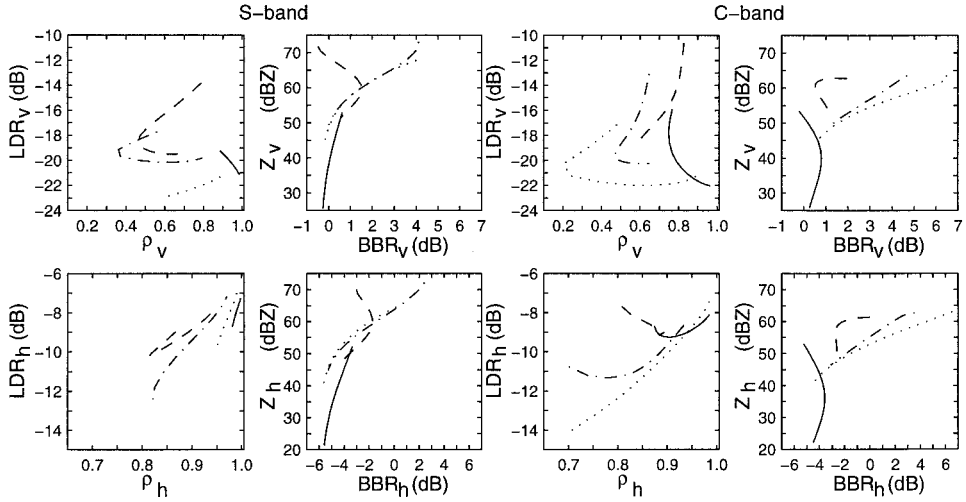

FIG. 6. S- and C-band bistatic radar parameters pairs for rain (solid line), dry hail (dotted line), slightly wet hail (dot–dashed line), and wet hail (dashed line). The incidence and scattering angles are $\theta_i = 95°$, $\phi_i = 180°$, and $\theta_s = 105°$, $\phi_s = 60°$.

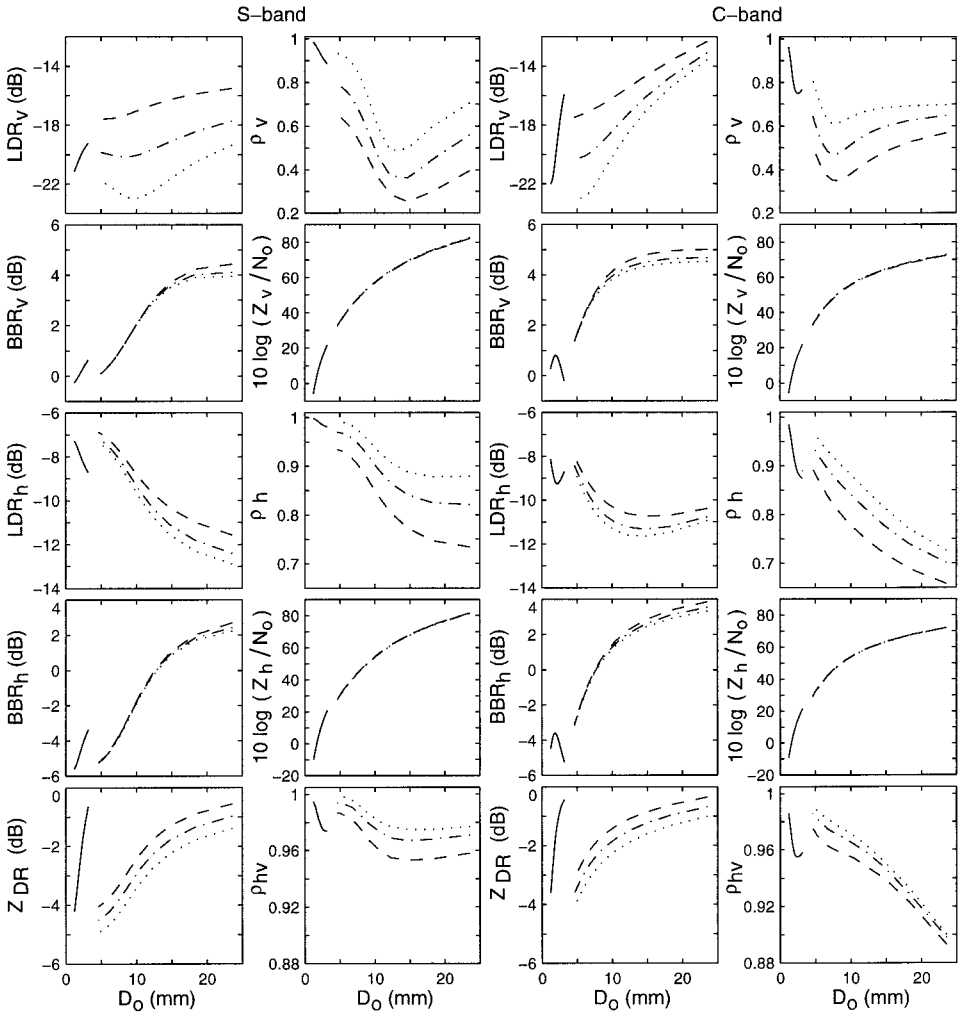

FIG. 7. S- and C-band bistatic radar parameters for v- and h-polarized transmission as a function of the median volume diameter D_0 for an exponential size distribution. The incidence and scattering angles are $\theta_i = 95°$, $\phi_i = 180°$, and $\theta_s = 105°$, $\phi_s = 60°$. The curves correspond to rain (solid line), hail with axial ratio 0.9 (dotted line), hail with axial ratio 0.8 (dot–dashed line), and hail with axial ratio 0.7 (dashed line). The hail is slightly wet (10% water–90% ice).

some cases (e.g., at S band for wet hailstones) the same value of BBR_v (or BBR_h) may lead to two different D_0 values. Assuming that D_0 can be obtained, one can determine the ratio Z_v/N_0 or Z_h/N_0 (see Figs. 4–7) and, knowing Z_v or Z_h, this will lead to an estimate of N_0.

Although not shown here, the general behavior and sensitivities noted for all of these bistatic radar parameters are similar at other incidence and scattering angles such as $\theta_i = 91°$, $\theta_s = 91°$, 100°, 110°, and $\theta_i = 110°$, $\theta_s = 100°$, 110°, and 120°. As indicated in the previous section, the single scattering results should provide insight into the variability of these parameters for other combinations of angles as well.

6. Conclusions

S- and C-band bistatic dual-polarization radar parameters were simulated in rain and hail to evaluate their potential use in differentiating the two precipitation types and estimating the parameters of an exponential size distribution for hail. Oblate spheroidal shape models together with canting distributions were used for raindrops and hailstones. Melting hailstones were simulated with several different mixtures of water and ice. For single-polarized transmission there are four parameters that may be useful for the purposes stated above; these are Z_v and the ratio parameters BBR_v, LDR_v, and ρ_v for v-polarized transmission. A similar set exists for h-polarized transmission. However, there may be limitations to using h-polarization due to low signal levels near the azimuth angle of 90° at low elevation angles for raindrops and small hailstones. In the case of dual-polarized transmission, both the v- and h-polarization sets plus the ratio parameters Z_{DR} and ρ_{hv} would be available. All of these parameters show significant vari-

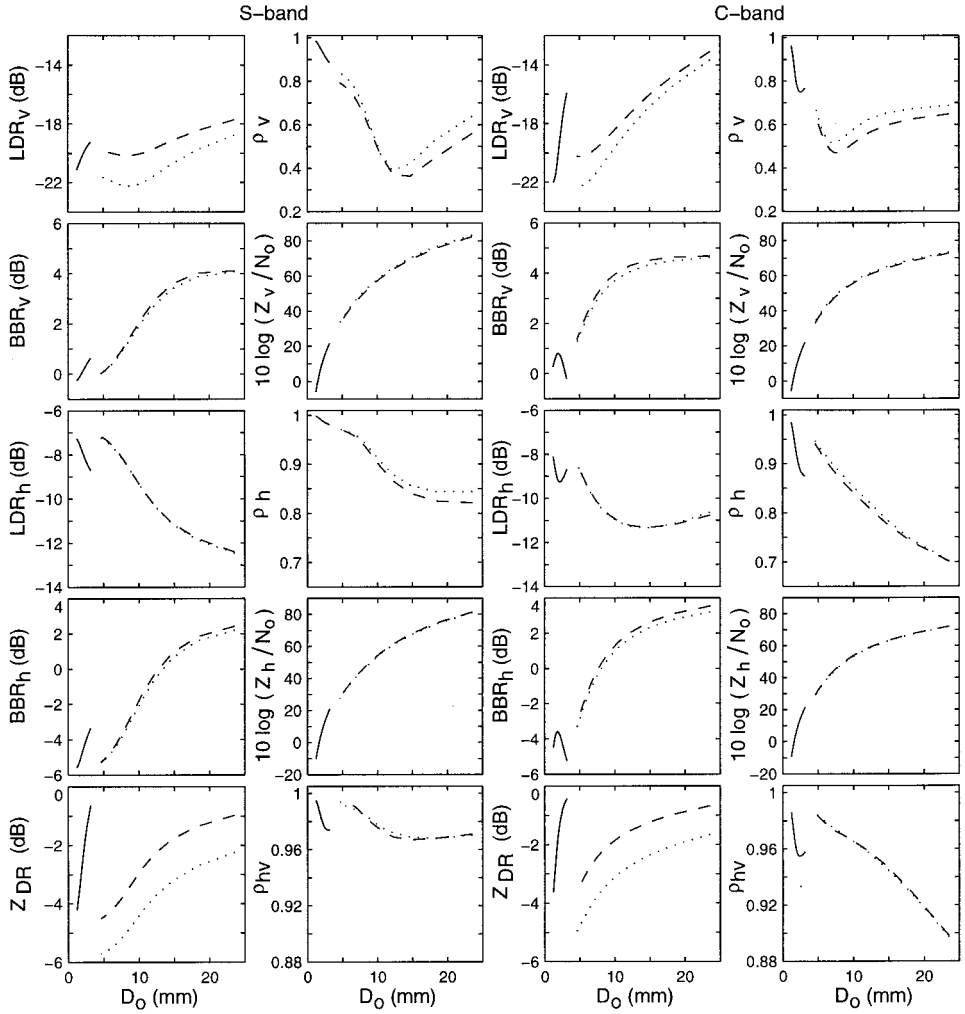

FIG. 8. S- and C-band bistatic radar parameters for v- and h-polarized transmission as a function of the median volume diameter D_0 for an exponential size distribution. The incidence and scattering angles are $\theta_i = 95°$, $\phi_i = 180°$, and $\theta_s = 105°$, $\phi_s = 60°$. The curves correspond to rain (solid line), hail with mean canting angle along the horizontal plane (dotted line), and hail with mean canting angle along the vertical direction (dashed line). The hail is slightly wet (10% water–90% ice) with axial ratio 0.8.

ability with the incidence and bistatic angles. They are also significantly affected by the amount of liquid water in melting hailstones, which may be useful for estimating the height where melting begins. The least affected parameters from changes in the axial ratios for hailstones are BBR_v, BBR_h, Z_v, and Z_h. All of the parameters except LDR_v, ρ_v, and Z_{DR} are negligibly affected by a change in the orientation model for hailstones (i.e., rotating the symmetry axis by 90°).

It was shown that rain and hail may be differentiated by observing them on radar parameter planes where they tend to cluster in different regions. Examples of these planes include LDR_v–ρ_v and BBR_v–Z_v for v-polarized transmission, and a similar set for h-polarized transmission, plus Z_{DR}–ρ_{hv} for dual-polarized transmission. Other combinations of these parameters also lead to similar results. Using more than one pair of parameters and/or several different bistatic receiver locations may enhance the level of confidence in the discrimination process. It should be noted that on some of these planes there are regions where rain and hail overlap; as a result, their discrimination may not always be possible.

For an exponential size distribution all the ratio parameters depend on the median volume diameter D_0 and not on N_0. Assuming that one knows the amount of water and ice in the hailstones (which may be difficult to determine except for hail that has not started melting), any one of the ratio parameters may be used for estimating D_0 over a limited size range. However, BBR_v and BBR_h appear to be the most promising ones due to their insensitivity to axial ratio and orientation. In some cases though (e.g., at S band for wet hailstones), BBR_v and BBR_h may lead to two different values of D_0, which may not always be resolvable even with the aid of other

parameters. If it is possible to estimate D_0, then N_0 can be obtained using Z_v or Z_h.

Acknowledgments. This work was supported by the National Science Foundation under Grant ATM-9225116 at The Pennsylvania State University.

REFERENCES

Atlas, D., K. Naito, and R. E. Carbone, 1968: Bistatic microwave probing of a refractively perturbed clear atmosphere. *J. Atmos. Sci.,* **25,** 257–268.

Awaka, J., and T. Oguchi, 1982a: Bistatic radar reflectivities of Pruppacher-and-Pitter form raindrops at 14.3 and 5.33 GHz. *J. Radio Res. Lab.,* **29,** 125–150.

——, and ——, 1982b: Bistatic radar reflectivities of Pruppacher-and-Pitter form raindrops at 34.8 GHz. *Radio Sci.,* **17,** 269–278.

Aydin, K., and Y. Zhao, 1990: A computational study of polarimetric radar observables in hail. *IEEE Trans. Geosci. Remote Sens.,* **28,** 412–422.

——, and S. H. Park, 1996: Simulation of dual-polarization bistatic scattering from rain and hail. *Proc. IGARSS'96,* Lincoln, NE, IEEE, 560–562.

——, T. A. Seliga, and V. Balaji, 1986: Remote sensing of hail with a dual linear polarization radar. *J. Climate Appl. Meteor.,* **25,** 1475–1484.

——, Y. Zhao, and T. A. Seliga, 1990: A differential reflectivity radar technique for measuring hail: Observations during the Denver hailstorm of 13 June 1984. *J. Atmos. Oceanic Technol.,* **7,** 104–113.

Balakrishnan, N., and D. S. Zrnić, 1990a: Estimation of rain and hail rates in mixed-phase precipitation. *J. Atmos. Sci.,* **47,** 565–583.

——, and ——, 1990b: Use of polarization to characterize precipitation and discriminate large hail. *J. Atmos. Sci.,* **47,** 1525–1540.

Battan, L. J., 1973: *Radar Observation of the Atmosphere.* University of Chicago Press, 324 pp.

Bohren, C. F., and L. J. Battan, 1982: Radar backscattering of microwaves by spongy ice spheres. *J. Atmos. Sci.,* **39,** 2623–2628.

——, and D. R. Huffman, 1983: *Absorption and Scattering of Light by Small Particles.* Wiley and Sons, 530 pp.

Bringi, V. N., T. A. Seliga, and K. Aydin, 1984: Hail detection with a differential reflectivity radar. *Science,* **225,** 1145–1147.

——, R. M. Rasmussen, and J. Vivekanadan, 1986a: Multiparameter radar measurements in Colorado convective storms, Part I: Graupel melting studies. *J. Atmos. Sci.,* **43,** 2545–2563.

——, J. Vivekanandan, and J. D. Tuttle, 1986b: Multiparameter radar measurements in Colorado convective storms, Part II: Hail detection studies. *J. Atmos. Sci.,* **43,** 2564–2577.

Cheng, L., and M. English, 1982: Hailstones concentration and size at the ground and the melting level. Preprints, *Conf. on Cloud Physics,* Chicago, IL, Amer. Meteor. Soc., 423–426.

Chylek, P., 1977: Depolarization of electromagnetic radiation scattered by nonspherical particles. *J. Opt. Soc. Amer.,* **67,** 175–178.

Crane, R. K., 1974: Bistatic scatter from rain. *IEEE Trans. Antennas Propag.,* **22,** 312–320.

Dibbern, J., 1987: Dependence of radar parameters on polarization properties of rain for bistatic CW radar. *Radio Sci.,* **22,** 769–779.

Doviak, R. J., and C. M. Weil, 1972: Bistatic radar detection of the melting layer. *J. Appl. Meteor.,* **11,** 1012–1016.

——, and D. S. Zrnić, 1993: *Doppler Radar and Weather Observations.* 2d ed. Academic Press, 562 pp.

Eccles, P., and P. Rogers, 1968: Relationship between rainfall rate and other measurable parameters of precipitation, the bistatic radar equation. Preprints, *13th Conf. on Radar Meteorology.* Montreal, PQ, Canada, Amer. Meteor. Soc., 364–369.

Goddard, J. W. F., S. M. Cherry, and V. N. Bringi, 1982: Comparison of dual-polarization radar measurements of rain with ground-based disdrometer measurements. *J. Appl. Meteor.,* **21,** 252–256.

Green, A. W., 1975: An approximation for the shapes of large raindrops. *J. Appl. Meteor.,* **14,** 1578–1583.

Illingworth, A. J., J. W. F. Goddard, and S. M. Cherry, 1986: Detection of hail by dual-polarization radar. *Nature,* **320,** 431–433.

Jameson, A., 1985: On deducing the microphysical character of precipitation from multiple-parameter radar polarization measurements. *J. Climate Appl. Meteor.,* **24,** 1037–1047.

Joss, J., J. C. Thams, and A. Waldvogel, 1968: The variation of raindrop size distributions at Locarno. *Proc. Int. Conf. on Cloud Physics,* Toronto, ON, Canada, Amer. Meteor. Soc., 369–373.

Knight, C. A., and N. C. Knight, 1970: The falling behavior of hailstones. *J. Atmos. Sci.,* **27,** 672–681.

Knight, N. C., 1986: Hailstone shape factor and its relation to radar interpretation of hail. *J. Climate Appl. Meteor.,* **25,** 1956–1958.

Kry, P. R., and R. List, 1974: Angular motions of freely falling spheroidal hailstone models. *Phys. Fluids,* **17,** 1093–1102.

List, R., U. W. Rentsch, A. C. Byram, and E. P. Lozowski, 1973: On the aerodynamics of spheroidal hailstone models. *J. Atmos. Sci.,* **30,** 653–661.

Matson, R. J., and A. W. Huggins, 1980: The direct measurement of the sizes, shapes and kinematics of falling hailstones. *J. Atmos. Sci.,* **37,** 1107–1125.

Olsen, R. L., and U. H. W. Lammers, 1978: Bistatic radar measurements of ice-cloud reflectivities in the upper-troposphere. *Electron. Lett.,* **14,** 219–221.

Park, S. H., 1996: Simulations of dual-polarization bistatic scattering from rain and hail. M.S. thesis, Dept. of Electrical Engineering, The Pennsylvania State University, 123 pp.

Ray, P. S., 1972: Broadband complex refractive indicies of ice and water. *Appl. Opt.,* **11,** 1836–1844.

Roos, D. V. D. S., and A. E. Carte, 1973: The falling behavior of oblate and spiky hailstones. *J. Rech. Atmos.,* **7,** 39–52.

Seliga, T. A., and V. N. Bringi, 1976: Potential use of radar reflectivity measurements at orthogonal polarizations for measuring precipitation. *J. Appl. Meteor.,* **15,** 69–76.

——, and ——, 1978: Differential reflectivity and differential phase shift: Applications in radar meteorology. *Radio Sci.,* **13,** 271–275.

Shupyatsky, A. B., 1974: Echo depolarization as measured with bistatic radar. *J. Rech. Atmos.,* **8,** 201–204.

Vivekanandan, J., V. N. Bringi, and R. Raghavan, 1990: Multiparameter radar modeling and observations of melting ice. *J. Atmos. Sci.,* **47,** 549–564.

Waterman, P. C., 1969: Scattering by dielectric obstacles. *Alta Freq.,* **38,** 348–352.

Wurman, J., 1994: Vector winds from a single-transmitter bistatic dual Doppler radar network. *Bull. Amer. Meteor. Soc.,* **75,** 983–994.

——, S. Heckman, and D. Boccippio, 1993: A bistatic multiple-Doppler network. *J. Appl. Meteor.,* **32,** 1802–1814.

——, M. Randall, C. L. Frush, E. Loew, and C. L. Holloway, 1994: Design of a bistatic dual-Doppler radar for retrieving vector winds using one transmitter and a remote low-gain passive receiver. *Proc. IEEE,* **82,** 1861–1872.

Zrnić, D. S., N. Balakrishnan, C. L. Ziegler, V. N. Bringi, K. Aydin, and T. Matejka, 1993a: Polarimetric signatures in the stratiform region of a mesoscale convective system. *J. Appl. Meteor.,* **32,** 678–693.

——, V. N. Bringi, N. Balakrishnan, K. Aydin, V. Chandrasekar, and J. Hubbert, 1993b: Polarimetric measurements in a severe hailstorm. *Mon. Wea. Rev.,* **121,** 2223–2238.